Interplay of structural, electronic, and magnetic properties of doped CdS

Edgar Ramirez

May 2024

Abstract

II/VI-type semiconductors, such as Cadmium Sulfide, are widely researched for their intriguing properties exhibited by the introduction of impurities in the crude structure. In this study, CdS was investigated through VASP calculations employing various approximations to determine the different effects of introducing main group element impurities in the material., such as the band gap, absorption, magnetic properties, etc. The goal of introducing various impurities, or doping, was to observe the unique properties exhibited by the doped material considering the various applications and uses, such as photovoltaic cells, optoelectronics (LEDs, laser diodes, etc.), pigments, photoresistors, gas sensors, etc. The impurity concentrations were examined for both structures of CdS, (WZ) and (ZB), with lattice parameters a = 4.136 Å and c = 6.714 Å for (WZ) and a = 5.819 Å for (ZB). A magnetic moment was measured in the lower concentration cells for most dopant atoms due to the increased distance between the impurities, thereby diminishing the impurity-coupled interactions; hence, maximizing the magnetic moment. Notably, nitrogen appeared to be the only dopant that had a suppressed magnetic moment due to the stronger interactions between it and the surrounding atoms. These findings demonstrate the intricate interactions between the dopant and pure atoms and the effect it has on the material's properties such as the band structure.

1 Introduction

Cadmium sulfide is an inorganic salt that exhibits two different crystal structures (see Figure 1 and 2): hexagonal wurtzite (WZ) and cubic zincblende (ZB). The choice between the two lattices determines the materials' various properties and applications, e.g. differences in the symmetry of the two structures, symmetrical (ZB) and unsymmetrical (WZ), results in variation in the band structure; band gap for (WZ) and (ZB) is 2.4 eV and 1.7 eV, respectively. Based on the total energy minimization approach, we note how the wurtzite structure is the predominant state and the ground state structure under normal conditions [2], with a band gap of 2.4 eV. Of the two structures, the wurtzite structure is the

most stable configuration [3], stemming from the hexagonal-closest packed (hcp) geometry. The closely packed atoms arranged in the hexagonal configuration maximize the packing efficiency, aiding in minimizing empty spaces in the lattice and reducing the overall energy of the system; hence, the (WZ) structure has a lower energy than the (ZB) structure. The total energy minimization approach entails finding a specific arrangement of atoms that results in the total energy of the lattice being minimum, starting from an initial configuration determined by experimental data. The total energy is first calculated using density functional theory (DFT), followed by adjustments in atom positions to minimize the energy of the system. Once the total energy is determined, we can proceed to minimize the total energy to determine the ground state. From [4], we have the following experimental lattice parameters a = 4.136 Å and c = 6.714 Å for the wurtzite structure. The lattice parameters, despite their seemingly subtle nature, play a major role in determining the various properties of these materials. Minimal changes in the lattice parameters drastically affect the band structure of CdS, which has a direct effect on the electrical conductivity and optical absorption. Furthermore, mechanical changes are also a direct result of sensitive changes in the parameters. This changes the interatomic distance between the two atoms, which influences the bond strength; hence resulting in changes in various mechanical properties e.g. mechanical strength, stiffness, elastic constants, etc. Furthermore, when the same wurtzite structure is under 2.7 GPa, it is transformed into the zincblende structure [5], where the atoms are arranged in a face-centered cubic (fcc) configuration with experimental lattice parameter 5.819 Å. This deformation changes various aspects of the structure; its experimental band gap energy is found to be 1.7 eV. The difference in band gap energy is a result of the different orbital characters exhibited by the zincblende states (p-d and s states), where the presence of more s-characters in Cd and S atoms is a result of the fcc configuration with alternating layers of Cd and S ions. Consequently, there is a weakened repulsion between the conduction and valence bands, and the band gap is diminished slightly [6]. article graphicx

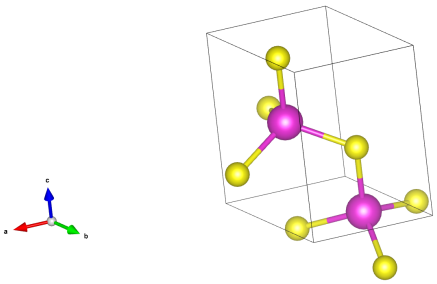

Figure 1: (a) WZ

article graphicx
In addition to the innate properties impacted by the varying lattice param-

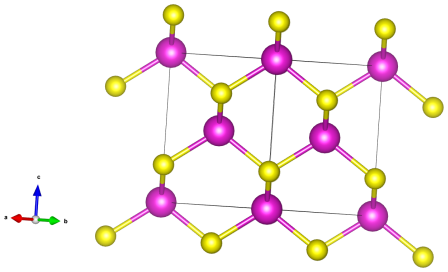

Figure 2: (b) ZB

Structure (CdS)	Dimensions (Å)	Number of atoms
ZB	8.25 x 8.25 x 8.25	16
ZB	11.66 x 11.66 x 11.66	64
WZ	8.32 x 8.32 x 6.77	16
WZ	12.48 x 12.48 x 13.51	72

Table 1: Dimensions and cell size used to simulate different impurity concentrations on CdS

eters, doping the lattice structure of CdS with main group elements (e.g. C, B, N, Al, Si, Ge, Ga) adds an additional layer of complexity to the properties and behavior. Doping is referred to as the addition of an impurity into the undoped lattice, varying in impurity concentrations depending on the size and dimensions of the structure used (see Table 1.). When we dope a pure structure with an impurity such as Aluminum—which doesn't have enough electrons to form 4 bonds with the structure—this doped structure is a p-type semiconductor, with the presence of holes because of dopant atom accepting electrons, leaving a positive charge (hole). These vacancies can be moved around the structure, which is how conductivity increases in the structure. An n-type semiconductor is one in which the dopant in the structure has excess electrons, hence, being the source of conductivity through the movement of unbonded electrons in the conduction zone. In our case, the lattice of interest is the carbon doped structure, which could be either an n-type or p-type depending on factors such as impurity concentration, temperature, the crystal structure, etc. Furthermore, the type of doping being investigated is known as anion doping, where the sulfur anion is replaced by a dopant molecule. Cation doping involves substituting cadmium by a dopant. In the present work, simulations of different impurity concentrations were constructed using varying dimensions to simulate different concentrations based on the number of dopant atoms per pure CdS atoms.

In each supercell seen in Table 1, one sulfur atom is replaced by the main group impurities. Lower impurity concentrations were performed on a 64 and 72-atom supercells for (ZB) and (WZ), respectively. Higher impurity concentrations were performed on a 16-atom supercell for both (ZB) and (WZ). In

the simulation of the 16 and 64-atom (ZB) supercell, the atoms interact with the impurities and are coupled (can interact with nearing neighbors) due to the proximity between the two. More specifically, the 3 interactions that are present are the interaction between the impurities, interaction between the impurities and nearest neighbor (NN = Cd), and interaction between impurities and next nearest neighbor (NNN = S). These interactions result in a wider impurity band, especially in higher dopant concentrations where the interactions are more prevalent. Furthermore, the presence of a wide impurity band can enhance the conductivity of the material [7]. Results show that only the carbon-doped CdS manifested a magnetic moment in second period substitutions (i.e. B, C, N), a consequence due to the holes introduced into the system (absence of an electron in atom - positive charge). This results in the p-bands in carbon to split magnetically, resulting in a magnetic moment of 2 µB. Similarly, for Si and Ga substitutions, two holes were introduced which also gave rise to a magnetic moment. When simulating the wurtzite structure of CdS, the same simulations were performed but on the 16 and 72-atom (WZ) supercells (Table. 1 for dimensions), simulating high and low concentration, respectively. The outcome of the calculations on the carbon doped structure were similar to that of the (ZB) structure, where a magnetic moment is present due to stronger spin polarization observed in carbon-like compounds of light nature. Results showed that as the distance between the NN/NNN and dopants increases, there is a corresponding diminishing amount the coupled interactions between the impurities, which explains the magnetic moment found in most systems other than nitrogen doped.

2 History of Density Functional Theory (DFT)

Density functional theory (DFT) is a popular technique used across multiple disciplines such as computational chemistry, biology, and solid-state physics in the investigation of the electronic structure of complex systems and the various properties they exhibit. It was introduced in 1964, where two physicists: Pierre Hohenberg and Walter Kohn, published a paper where they proposed that the correlation and exchange energies in systems of uniform electron gas density (LDA) can be approximated from the total electron density [8]. It all happened when they met each other and worked together to develop the now known Hohenberg-Kohn (HK) theorem in DFT, which is used to determine the ground state from the electron density. About a year after the publication of HK, Kohn along with his student, Lu Sham, formulated the Kohn-Sham (KS) equations. The equations aim to determine the exchange-correlation (XC) potential E/(r), where the exchange describes the effect associated with placing two electrons of the same spin in the same region (comes from Pauli exclusion principle), and the correlation considers the repulsive nature of electrons because of the coulombic interaction.

Over the following decades, several XC functionals were developed to further improve the calculations for the XC energy, all varying in computational

difficulty and the accuracy of the results, which can often be conceptualized by Jacob's ladder of DFT. As we ascend the ladder—starting with LDA, followed by the more sophisticated GGA, which introduces the gradient of the electron density , meta-GGA, which is an extension of GGA by taking the Laplacian of the electron density 2, hybrid functionals, such as HSE06, and double hybrid functionals—we obtain better approximations from the one's trailing behind. Additionally, the self-consistent interaction that arises due to the interacting d and f electrons in calculations in GGA and LDA can be avoided by the addition of the Hubbard constant U [9]. This additional term cancels out the self-consistent interaction energy, which yields accurate results for the defect formation energy. These are just a few of the many reasons which make DFT superior to Hartree-Fock (HF), since they don't consider the electron-electron interactions, completely neglecting the Pauli exclusion principle. The HF method in determining the ground state is found by solving the many-body Schrodinger equation from approximating the wavefunction as a single determinant i.e. the HF wavefunction. This results in an underestimation of the HF energy, which can be trivial in certain cases where the system exhibits electron-electron interactions such as atoms and molecules interacting via coulombic forces, high temperature superconductors, certain magnetic materials, etc.

3 Computational Methods

In simulating the various CdS structures, VASP was used in the performance of the various calculations to modify our desired structure, along with various different functionals. The approximation of interest is the Heyd-Scuseria-Ernzerhof (HSE) approximation, which avoids the common pitfall of the generalized gradient approximation (GGA) which comes with false occupancies i.e. false ferromagnetism. HSE06 has been shown to produce more accurate results over GGA and local density approximation (LDA), producing more accurate calculations for the band-gap energy; hence, giving a more accurate representation of the semiconductor and its properties [10]. The advantages and disadvantages of the different DFT functionals depends on the quantity being investigated. LDA is advantageous when dealing with systems of uniform electron density, where the spatial variation of the XC energy density can be neglected. Such systems could include simulations of bulk materials (i.e. metals, semiconductors, etc.) and simple molecules (hydrocarbons or diatomic molecules). Nonetheless, HSE06 provides strikingly accurate results in electronic structure calculation, i.e. the bandgap energy calculated provides much closer approximation to the literature value of the bandgap compared to LDA and GGA. Regardless, the structures were relaxed (i.e. optimized to determine most stable configuration) using GGA, followed by several modifications performed within VASP to further optimize the structure. Atomic positions were allowed to change during the simulation, as well as changes in cell dimensions to simulate different impurity levels. Before experimenting with the dopant system, the Perdew-Burke-Ernzerhof (PBE) approximation (type of GGA) was used on undoped CdS to obtain references

Impurity	(ZB), 16 cell	(ZB), 64 cell	(WZ) 16 cell	(WZ) 72 cell
B	3.00	3.00	1.75	3.00
C	2.00	2.00	2.00	2.00
N	0.75	0.81	0.70	0.75
Al	1.25	3.00	1.00	3.00
Si	2.00	2.00	1.00	1.00
P	1.00	1.00	1.00	1.00
Ga	1.47	3.00	1.25	3.00
Ge	2.00	2.00	0.75	2.00

Table 2: Magnetic moment (µB) calculated using HSE06

that can be used to compare to the doped structure. The obtained structure was then processed using HSE06, with the addition of the dopant atom to yield the results (see Table 3.).

4 Results

4.1 Structural Parameters

The structural parameters are important features in investigating CdS. For (WZ) CdS, the chosen lattice parameters are a = 4.136 Å and c = 6.714 Å; for (ZB) CdS, the chosen lattice parameter is a = 5.819 Å. Their specific arrangement determines the various properties of each crystal structure. For instance, the spacing between each atom is determined by the lattice parameters, which affects the strength of the bonds and bond length. These spacing influences the band structure, due to changes in the hybridization and orbital overlap, affecting properties such as conductivity, bandgap, and optical absorption. This is especially important when considering the introduction of impurities, since this can result in changes in the spatial distribution of the dopant and altering their interactions with the charge carriers.

4.2 Magnetic Properties

From Table 2., we note how the magnetic moments obtained for the two different structures using HSE06 are quite similar, despite the (WZ) values being an approximation given that the results were interpreted graphically. From this, we can confirm that the magnetic moment isn't affected by the lattice structure; hence, our calculations can be performed on the symmetrical (ZB) structure. This helps avoid the tedious calculation of the non-local Fock exchange integral. However, the lattice parameters noticeably affect the magnetic moment. As seen in both structures, (WZ) and (ZB), the lower impurity concentration cell displays a stronger magnetic moment than the higher impurity concentration cell. This phenomenon arises from various factors, notably the weakened interaction between other impurities and the pure atoms, and the increased dis-

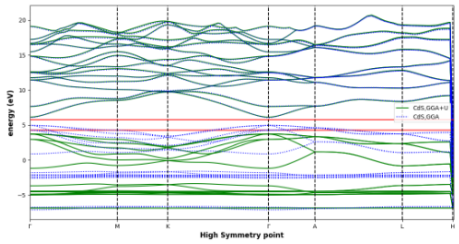

Figure 3: Comparative display of GGA (blue) and GGA+U (green) band structure of pure CdS (WZ)

tance between dopant atom and their surroundings. This reduced interaction and greater separation allows for a more pronounced magnetic moment without getting damped as a result of coupled interactions with dopant atoms and their surroundings, as is the case in higher impurity concentration cells.

4.3 Band Structure

The band structure is a key factor that must be analyzed to determine the bandgap of the material. This property was determined for the undoped (WZ) structure (see Figure 3) using GGA and GGA+U [11], in which a comparative study was conducted between the band structure calculated using GGA and GGA+U to demonstrate how DFT+U method is superior in specific cases. This, of course, is a result of the ignorance of the self-interaction term, which was corrected using the Hubbard parameter. The band gap obtained using GGA and GGA+U is 1.10 eV and 2.40 eV, respectively. The values used were Ud = 4.5 and Up =4.2 for Cd-d and S-p orbitals, respectively. This results in a band gap of 2.4 eV, which is a significant improvement over the 1.10 eV obtained using GGA. As seen in the band structure, there is a downward shift in the valance band maxima when using GGA+U, which is reflected in the band gap calculations. The conduction band remains the same for both methods; where we note the upper conduction band consists of the Cd-p orbitals and the lower conduction band consists of S-p orbital. Moreover, when determining the bandgap of the doped structure, it is well known that such approximations on doped systems would bring rise to various inaccuracies since the orbitals are delocalized. Consequently, electrons flow freely through the structure with nonuniform electron density, causing faulty ferromagnetism. This also results in an underestimation of the bandgap, which is important in determining the properties; hence, HSE06 was the chosen approximation used to calculate the band-gap energy. However, hybrid functionals come at a computational cost with a much slower rate to obtain results. HSE06 also requires additional calculations for the (WZ) structure of CdS, primarily because of its a less symmetrical structure, requiring the calculation of the non-local Fock exchange integral to account for the coulombic repulsion between electrons in different regions of the

Cell Size	GGA (eV)	HSE (eV)	Literature Value (eV)
WZ CdS	1.11	2.16	2.4 [4]
ZB CdS	1.05	2.06	1.7 [4]

Table 3: Caption

lattice (long range interactions).

4.4 Density of States (DOS) and Partial DOS

The Density of States (DOS) was also an important quantity that was investigated, which is important when discussing the magnetic behavior of doped systems. The band structure determines the overall shape and characteristics of the DOS, e.g. the peaks in the DOS correspond to energy levels/bands in the band structure with a high concentration of electron density. For second period substitutions (C, B, N), carbon was the only dopant seen to exhibit magnetic moment as a direct result of the Fermi energy lying within the peak of the DOS (see Figure 4.), because of the electron vacancies. These vacancies represent an energy level in the bandgap of the material where an electron could potentially be found. Furthermore, the interaction between the impurity states and the electron vacancies plays a major role in the shape of the DOS near the Fermi level. Impurity states arise because of doping, leading to hybridized states that resonate with the electron vacancies, which manifests in the formation of energy peaks within the DOS near the Fermi level. These peaks represent an area of higher electron density, where the electrons are more likely to be observed. This intense peak of the DOS near the Fermi energy satisfies the Stoner criteria (condition for ferromagnetism); consequently, the p-orbitals split magnetically, leading to the manifestation of a magnetic moment as seen in the case of carbon-doped CdS. This same reasoning can explain the magnetic moments observed when other dopants are used, as well as the unsaturated magnetic moment found in Silicon and Germanium in the higher concentration supercell due to the lower intensity of DOS at the Fermi level. In lower concentration supercells (64- and 72-atom), the increase in distance between impurities results in a diminishing of coupled interactions; consequently, increasing the magnetic moment of most dopant systems. Nitrogen was the exception to this, since its coupled interactions were still notable because of the proximity between the impurity and the NN; thus, diminishing the magnetic moment. Additionally, the partial and total density of states was determined, which are important factors in understanding the electronic structure and magnetic behavior of the doped CdS. The total density of states is broken down into the individual contributions of each specific atomic orbital (s, p, d, or f) in the structure being analyzed. In the carbon doped system, the coupling between the Sulfur p orbital and Cadmium d orbital resonates with the impurity. From Figure 4., we see how the carbon-p spins aren't degenerate (spins aren't aligned). This is displayed by the splitting of energy levels for spin-up and spin-down, which results in a magnetic moment

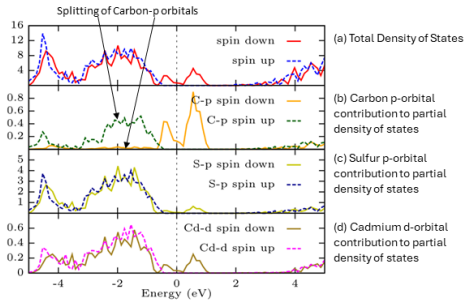

Figure 4: Total (a) and Partial DOS (b, c, d) of Carbon doped CdS

as seen in the case for C-doped CdS. The electron density is found to resonate around the Fermi level, which is a result of coupling interactions. Interestingly, the boron and aluminum doped systems in lower impurity concentration also exhibited a magnetic moment, resulting from the polarization of the valence band where, unlike the vanishing magnetic moment calculated in higher impurity concentrations. The dopant atom introduces electronic states within the band structure, which results in both magnetic and insulating properties, originating from the p-electrons. Additionally, the number of interactions that occur between the impurities and the neighboring atoms is significantly less than in the higher impurity concentration, which amplifies the magnetic moment.

4.5 Interplay of structural, electronic, and magnetic properties

As discussed previously, the structural parameters used directly affect the materials electronic and structural properties, such as the bandgap, DOS, band structure, etc. Furthermore, from the band structure, the conduction band minima can determine the materials conductivity and optical properties. Under incident light, photons with energy greater than the valance band maximum (h ¿= EVB) excite electrons from this band to the conduction band, which results in optical absorption [12]. This introduces photo-induced carriers —electrons or holes— which contribute to the electrical current produced by a photodiode in response to light (or photocurrent). If the incident light has an energy below the valence band maximum, then the corresponding energy is converted to electrical power and is still used to generate photo-inducted carriers and photocurrent. When considering the doped CdS, this transition occurs more readily since this introduces additional impurity levels, which allow electrons to transition to the conduction band more readily and the generation of photo-induced carriers. These excited electrons become entrapped in the impurity levels, which contributes to the photocurrent. As expected, introducing impurities alters the electronic properties, such as the bandgap, of the structure, which explains the lower responsivity and operating speed of the material. In-

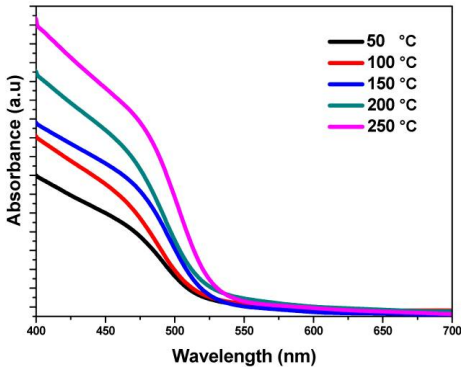

Figure 5: Temperature dependence of absorption in CdS films

terestingly, the magnetic properties arising from introduction of impurities in CdS influence the excitonic behavior of the material, which reveals a lot about its optical properties. An exciton is a bound state of an electron and a hole, formed due to their coulombic interaction, where the collective interaction of these excitons is called a quasiparticle. An electron in the conduction band can recombine with a hole in the valence band, which causes the emission of a photon. Moreover, it is well known that for CdS, the photons emitted are in the visible spectrum when transitioning [13], more notably in larger wavelengths of lower frequency (500 – 520 nm). As seen in Figure 5, the temperature dependence of absorbance/transmittance in CdS films increases with increasing temperature and is shifted to a greater extent towards the visible range. This broadening in absorption in the visible spectrum can be attributed to the narrowing of the bandgap, allowing electrons in lower energy bands to transition more easily to the conduction band; hence, broadening of the range of absorbed wavelengths/photons. Moreover, alterations in the band structure due to doping result in shifts in the absorption and emission spectra of the material, which further narrows the bandgap and improves electron transitioning from the VB to the CB. Consequently, this broadens the absorption/transmission in the visible range, which is of particular interest in the photocatalytic H2 generation [14].

4.6 Defect Formation Energy (DFE)

Another additional value was calculated is the defect formation energy, which tells use the ease with which we can incorporate a dopant atom into the crude lattice. It takes various factors into account to determine the value; the total energy resulting from the replacement of sulfur with the dopant, the total energy of the undoped structure, the number of sulfur atoms replaced, and the chemical potentials of Cd and S. This value was calculated for both (WZ) and (ZB) in both high and low dopant concentration and the calculated DFEs gave very similar results, meaning that these values are independent of the lattice structure

since the structure doesn't influence the values. Interestingly, it was found that most of the DFEs were relatively low, except Aluminum and Gallium, with values greater than 4 eVs, which makes them more difficult to synthesize.

5 Conclusion

In the investigation of doping main group impurities into CdS, hybrid functional HSE06 predicted magnetic moments when CdS was doped with B, C, Si, P, and Ge at both high and low concentrations. A key finding is that the magnetic moment manifested due to the stabilization of the holes introduced through doping and their interaction with p-electrons, rather than through interactions with d-electrons. In Al and Ga doped structures, there is an unsaturated magnetic moment in higher impurity concentrations due to the lower extent of interactions between the impurities and the atoms, but still maintains insulating properties due to the fact the Al and Ga have stronger interactions with the atoms than the other dopant atoms. Additionally, the doping of such materials greatly affects its optical and electronic properties, which arises from the impurity levels introduced in the bandgap, which makes it easier for electrons to jump to the conduction band. Consequently, this broadens the absorption in the visible spectrum, more specifically, at the higher wavelengths in the region associated with red, more commonly referred to as the redshift. These various properties exhibited by crude CdS and doped CdS bring rise to several applications in the present and near future, including solar energy, optoelectronics, photocatalytic H2 generation, quantum dots, and myriad other applications.

6 References

[1] Ismail, Walid, et al. "Advancement of Physical and Photoelectrochemical Properties of Nanostructured Cds Thin Films toward Optoelectronic Applications." Nanomaterials (Basel, Switzerland), U.S. National Library of Medicine, 30 May 2023, www.ncbi.nlm.nih.gov/pmc/articles/PMC10254828/. [2] Wei, S H, and S B Zhang. "ZB/WZ Band Offsets and Carrier Localization in CdTe ... - NREL." National Renewable Energy Laboratory , 1 Jan. 2000, www.nrel.gov/docs/fy00osti/28291.pdf. [3] Prakash, Jai, et al. "CDs Based 3D Nano/Micro-Architectures: Formation Mechanism, Tailoring of Visible Light Activities and Emerging Applications in Photocatalytic H 2 Production, CO 2 Reduction and Organic Pollutant Degradation." Journal of Materials Chemistry A, Royal Society of Chemistry, 18 Apr. 2023, pubs.rsc.org/en/content/articlehtml/2023/ta/d3ta00396e. [4] Ankan Biswas, et al. "Electronisc and Band Structure Calculation of CdS Using GGA and GGA+ U Functionals." IOP Science, iopscience.iop.org/article/10.1088/1742-6596/2267/1/012155/pdf. Accessed 29 Mar. 2024. [5] Bedolla, P O, et al. "P-Electron Magnetism in CdS Doped with Main Group Elements." Journal of Physics: Condensed Matter, 2012, iopscience.iop.org/article/10.1088/0953-8984/24/47/476002/pdf. [6] Yeh, Chin-Yu, et al. "Relationships between the

Band Gaps of the Zinc-Blende ..." Physical Review B, 6 May 1994, www.colorado.edu/faculty/zunger-matter-by-design/sites/default/files/attached-files/231.pdf. [7] Nave, R. "Band Theory of Solids." Band Theory for Solids, hyperphysics.phy-astr.gsu.edu/hbase/Solids/band.html. Accessed 20 Apr. 2024. [8] Becke, Axel D. "Perspective: Fifty Years of Density-Functional Theory in Chemical Physics." AIP Publishing, AIP Publishing, 1 Apr. 2014, pubs.aip.org/aip/jcp/article/140/18/18A301/149389/Perspective-Fifty-years-of-density-functional [9] Edossa, Teshome Gerbaba, and Menberu Mengasha Woldemariam. "Electronic, Structural, and Optical Properties of Zinc Blende and Wurtzite Cadmium Sulfide (Cds) Using Density Functional Theory." Advances in Condensed Matter Physics, Hindawi, 20 Aug. 2020, www.hindawi.com/journals/acmp/2020/4693654/. [10] Moses, Poul Georg, et al. "Hybrid Functional Investigations of Band Gaps and Band Alignments for Aln, Gan, Inn, and Ingan." AIP Publishing, AIP Publishing, 25 Feb. 2011, pubs.aip.org/aip/jcp/article-abstract/134/8/084703/960261/Hybrid-functional-investigations-of-band-gaps-and?redirectedFrom=fulltext. [11] Ankan Biswas, et al. "Electronic and Band Structure Calculation of CdS Using GGA and GGA+ U Functionals." IOP Science, iopscience.iop.org/article/10.1088/1742-6596/2267/1/012155/pdf. Accessed 29 Mar. 2024. [12] Stateikina, Irina. "Optoelectronic Semiconductor Devices - Principals And ..." Science Direct, 17 Feb. 2002, mtf.etf.bg.ac.rs/downloads/dokumenti/Optoelectronic Semiconductor Devices - Principals and Characteristics.pdf. [13] Al-Hussam, Abdullah M.A, and Salah Abdul-Jabbar Jassim. "Synthesis, Structure, and Optical Properties of Cds Thin Films Nanoparticles Prepared by Chemical Bath Technique." Journal of the Association of Arab Universities for Basic and Applied Sciences, ScienceDirect, 13 Jan. 2012, www.sciencedirect.com/science/article/pii/S1815385211000356. [14] Zubair, Muhammad, et al. "Core-Shell Particles of C-Doped Cds and Graphene: A Noble Metal-Free Approach for Efficient Photocatalytic H2 Generation." Green Energy and Environment, Elsevier, 17 Oct. 2020, www.sciencedirect.com/science/article/pii/S246 Perverati, Roberto, and Donald G Truhlar. "Exchange–Correlation Functional with Good Accuracy for Both Structural and Energetic Properties While Depending Only on the Density and Its Gradient — Journal of Chemical Theory and Computation." ACS Publications, 10 July 2012, pubs.acs.org/doi/10.1021/ct3002656.